

Modelling infrared spectra of a few compact HII regions

S. K. Ghosh and R. P. Verma

Tata Institute of Fundamental Research, Homi Bhabha Road, Mumbai 400005, India

Abstract. The observed near infrared to sub-mm spectra of five compact HII regions, viz., IRAS 18116-1646, 18162-2048, 19422+2427, 22308+5812 and 18434-0242, consisting of the continuum as well as several features, have been explained well by radiative transfer through a spherical dust cloud. In addition to the equilibrium thermal emission from the normal dust grains (BG), the non-equilibrium processes, e.g. transient heating of the very small grains (VSG) as well as the Polycyclic Aromatic Hydrocarbon (PAH) are also taken into account by a novel scheme of segmenting the main cloud into individual "onion skin" cloud shells.

The following have been concluded about these compact HII regions : (i) the uniform radial density distribution gives an excellent fit to the entire body of the data (other cases e.g. r^{-1} , $r^{-1.5}$ or r^{-2} etc can be ruled out); (ii) the PAH features are predicted very well only if these molecules exist exclusively in the central region (a few % of radius) of the cloud; and (iii) the silicate grains constitute only 5-25% of the BG component (rest being graphite).

1. Introduction

With the advent of the Infrared Space Observatory (ISO), the entire infrared spectral energy distributions (SED) of Galactic compact HII regions are becoming available. In the present work, a new scheme of radiative transfer including in addition to the dust grains in thermal equilibrium, the transient heating of Very Small Grains (VSG) as well as Polycyclic Aromatic Hydrocarbons (PAH), has been developed. This has been successfully applied to five compact HII regions : IRAS 18116-1646, 18162-2048, 19442+2427, 22308+5812 and 18434-0242.

2. The Model

The spherically symmetric dust cloud, containing the embedded energy source (e.g. a ZAMS star), is divided into a large number of concentric contiguous spherical shells like "onion skins". In order to incorporate the presence of both - normal grains (Big Grains, BG, responsible for emission at thermal equilibrium), as well as the grains responsible for non-equilibrium emission (VSG and PAH), each shell is subdivided into a pair of sub-shells corresponding to these two components respectively. Radiative transport at each of the two sub-shells is carried

out as a two point boundary value problem, the two boundary conditions being the incident radiation fields at the two surfaces. Starting from the inner most shell, the radiation is transported through the successive shells, till the outer boundary of the cloud is reached. This entire processing constitutes one iteration. Typically 5-10 iterations are needed to achieve convergence.

The VSG and PAH components of grains have fluctuating temperature, mainly because their enthalpy (internal energy) is comparable to the energy of UV or visible photons. As a result, the multiphoton absorption processes lead to a modified temperature distribution. An iterative method has been used to consider these multiphoton processes. The method assumes a single grain in an isotropic radiation field, and follows the evolution of the grain temperature by solving the relevant stochastic differential equation (Desert et al., 1986).

A scheme of between 100 to 400 energy levels of internal energy (covering 0.5 eV to 200 eV) for considering discrete heating / cooling processes; and 400 energy levels (for photon energies 1.25×10^{-3} to 0.5 eV) for considering the continuum processes, has been incorporated.

Each of the sub-shells consisting of the normal grains, separately undergo full radiative transport calculation using the code CSDUST3 developed by Egan et al. (1998). In CSDUST3, the moment equation of radiation transport and the equation of energy balance are solved simultaneously as a two-point boundary value problem

We have chosen five out of the six sources for which the ISO-SWS spectra (6-12 μm) are published by Roelfsema et al. (1996). In addition to the ISO data, the IRAS PSC measurements (at 12, 25, 60 & 100 μm), IRAS LRS spectra between 8 - 22 μm and ground based 3.3 μm spectroscopy have been used.

The normal grains (BG) consist of two components : Astronomical Silicate and Graphite, each with a size distribution $n(a) \sim a^{-3.5}$ with a between 0.01 μm and 0.25 μm . The VSG component is taken to be graphite grains of a single size : either 10 \AA or 50 \AA in radius. The scattering and absorption coefficients for BG and VSG have been taken from Draine & Lee (1984) and Laor & Draine (1993). The PAH component is assumed to be either a single molecule with about 15 - 30 atoms, or a large complex consisting of 10 - 20 small molecules as used by Siebenmorgen (1993). Their optical properties have been taken from Leger & d'Hendecourt (1987).

It was found that the models with uniform density distributions (as opposed to $n(r) \sim r^{-1}$ or r^{-2}) gave much better fits to the SEDs. The VSGs with $a_{\text{VSG}} = 50 \text{\AA}$ and the PAHs with intermediate size (i.e. $a_{\text{PAH}} = 8 \text{\AA}$) give better fits to the respective spectra.

Whereas the BG and VSG components should exist throughout the cloud, it is necessary that the PAH component must be confined to a thin inner region quantified by, $\eta_{\text{PAH}} = ((R_{\text{out}}^{\text{PAH}} - R_{\text{in}}) / (R_{\text{out}} - R_{\text{in}}))$.

The values of the best fit parameters specific to each source, are presented in Table 1. The model calculated spectrum for the compact HII region IRAS 19442+2427 is compared with observations in Figure 1.

Table 1. Best fit parameters of the compact HII regions as determined by modelling.

IRAS Source Name	R_{in} (pc)	R_{out} (pc)	n_H (cm^{-3})	M_{Tot} (M_{\odot})	τ_{100}	Grp:Sil (% : %)	η_{PAH}
18116-1646	1.4×10^{-3}	1.12	1.32×10^4	1.9×10^3	0.056	75 : 25	2.1×10^{-2}
18162-2048	5.3×10^{-4}	0.29	1.32×10^5	3.3×10^2	0.14	88 : 12	2.7×10^{-2}
19442+2427	7.5×10^{-4}	0.52	5.30×10^4	7.7×10^2	0.10	95 : 5	1.5×10^{-2}
22308+5812	1.5×10^{-3}	1.31	1.38×10^4	3.2×10^3	0.068	77 : 23	1.3×10^{-2}
18434-0242	2.2×10^{-3}	0.69	5.30×10^4	1.8×10^3	0.14	95 : 5	5.5×10^{-2}

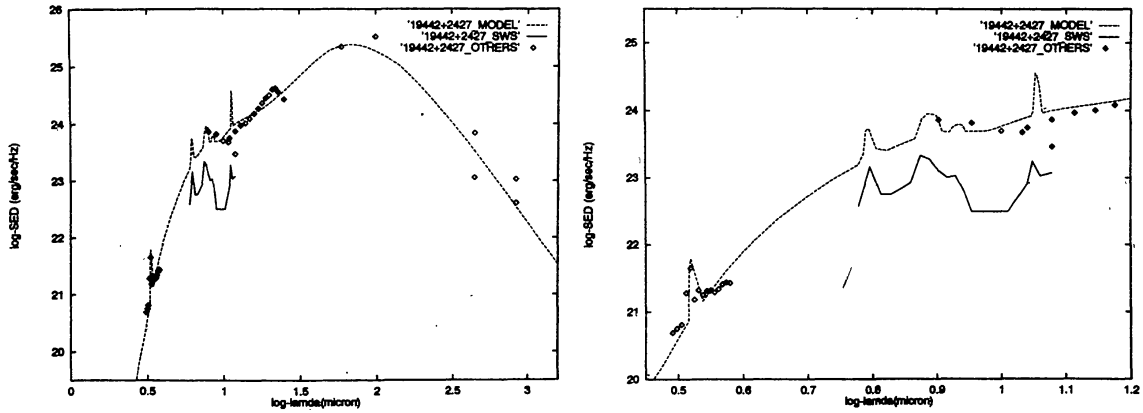


Figure 1. a,b Spectral energy distribution of the compact HII region IRAS 19422+2427. Solid line shows the ISO-SWS spectrum from Roelfsema et al. (1996); dotted line shows our best fit model spectrum; diamonds show other observations. Other observations include - 3 μm observations from Muizon et al. (1990), IRAS LRS spectrum from Volk & Cohen (1989), IRAS PSC flux densities, sub-mm observations from Jenness et al. (1995). In order to show the PAH features clearly, mid IR region of the SEDs are shown separately.

3. Results

The surprising results of the present work is that most favoured radial dust density distribution law, for all five sources, turns out to be of uniform density.

A quick perusal of Figure 1 and Table 1 brings out the following facts : (i) All the compact HII regions considered here, are deeply embedded stars; total optical depth at 100 μm in the range of 0.056 – 0.14. (ii) PAH is confined only to a thin central shell whose thickness is

just a few percent (1.3 – 5.5 %) of the total thickness of the dust cloud. (iii) The BGs are dominated by graphites, with silicates contributing less than 25 %. (iv) ISO-SWS fluxes are generally much smaller than IRAS LRS fluxes at similar wavelengths, indicating that SWS is not sampling full emission at mid IR. Another important outcome is that the relative abundance of graphite and astronomical silicate has been tied down rather precisely by the 10 μm silicate feature.

The present study has also excluded the possibility of the following geometry popular with YSOs : a disk very near the embedded star plus a far off spherical shell. Future studies must explore the disk like geometry, which may lead to equally good fit to the observed SED with more uniform mixing of PAH and the BGs.

Acknowledgement

It is a pleasure to thank Bhaswati Mookerjea for her help in preparing some input parameters.

References

- Desert F. X., Boulanger F., Shore S. N., 1986, *A&A*, 160, 295.
Draine B. T., Lee H. M., 1984, *ApJ*, 285, 89.
Egan M. P., Leung C. M., Spagna G. F., 1988, *Computer Physics Communications*, 48, 271.
Jenness T., Scott P. F., Padman R., 1995, *MNRAS*, 276, 1024.
Laor A., Draine B. T., 1993, *ApJ*, 402, 441.
Leger A., d'Hendecourt L., 1987, in "PAH and Astrophysics" eds. A. Leger, L. d'Hendecourt & N. Boccara, p. 223.
Mathis J. S., Rumpl W., Nordsiek K. H., 1977, *ApJ*, 217, 425.
Muizon M. de, d'Hendecourt L. B., Geballe T. R., 1990, *A&A*, 227, 526.
Roelfsema P. R., Cox P., Tielens A. G. G. M et al., 1996, *A&A*, 315, L289.
Siebenmorgen R., 1993, *ApJ*, 408, 218.
Volk K., Cohen M., 1989, *AJ*, 98, 931.